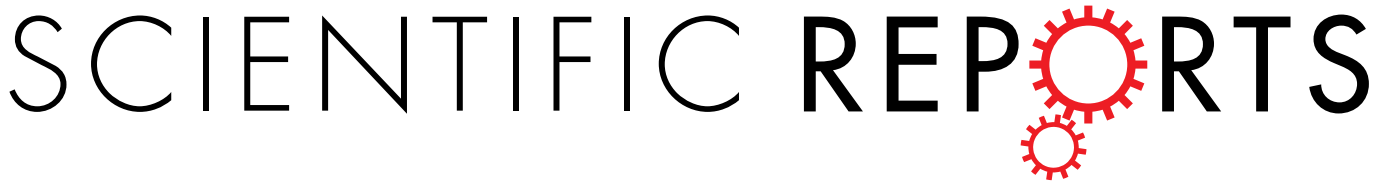

OPEN

Enhanced critical current density in the pressure-induced magnetic state of the high-temperature superconductor FeSe

Received: 15 June 2015
Accepted: 14 October 2015
Published: 09 November 2015

Soon-Gil Jung[1], Ji-Hoon Kang[1], Eunsung Park[1], Sangyun Lee[1], Jiunn-Yuan Lin[2], Dmitriy A. Chareev[3], Alexander N. Vasiliev[4,5,6] & Tuson Park[1]

We investigate the relation of the critical current density (J_c) and the remarkably increased superconducting transition temperature (T_c) for the FeSe single crystals under pressures up to 2.43 GPa, where the T_c is increased by ~8 K/GPa. The critical current density corresponding to the free flux flow is monotonically enhanced by pressure which is due to the increase in T_c, whereas the depinning critical current density at which the vortex starts to move is more influenced by the pressure-induced magnetic state compared to the increase of T_c. Unlike other high-T_c superconductors, FeSe is not magnetic, but superconducting at ambient pressure. Above a critical pressure where magnetic state is induced and coexists with superconductivity, the depinning J_c abruptly increases even though the increase of the zero-resistivity T_c is negligible, directly indicating that the flux pinning property compared to the T_c enhancement is a more crucial factor for an achievement of a large J_c. In addition, the sharp increase in J_c in the coexisting superconducting phase of FeSe demonstrates that vortices can be effectively trapped by the competing antiferromagnetic order, even though its antagonistic nature against superconductivity is well documented. These results provide new guidance toward technological applications of high-temperature superconductors.

The technological application of superconductors hinges on how to preserve a zero-resistance state at high temperature while maintaining large electrical currents. The discovery of copper-based high-temperature superconductors (HTSs) brought great excitement not only because of its unconventional superconducting nature, but also because of its high superconducting transition temperature (T_c), which was expected to open the door for revolutionary applications at temperatures higher than liquid nitrogen temperature (=77 K) (refs 1–3). A key issue for practical applications of superconductors is the necessity to increase the value of the depinning critical current density (J_c), at which magnetic flux lines (or vortices) start to flow and energy dissipation occurs. For decades, several approaches effectively enhanced the J_c of HTSs by introducing and/or manipulating the extrinsic defects that suppress superconductivity[4,5]. Because the

[1]Department of Physics, Sungkyunkwan University, Suwon 440-746, Republic of Korea. [2]Institute of Physics, National Chiao Tung University, Hsinchu 30010, Taiwan. [3]Institute of Experimental Mineralogy, Russian Academy of Sciences, Chernogolovka, Moscow Region 142432, Russia. [4]Low Temperature Physics and Superconductivity Department, Physics Faculty, Moscow State University, 119991 Moscow, Russia. [5]Theoretical Physics and Applied Mathematics Department, Institute of Physics and Technology, Ural Federal University, Ekaterinburg 620002, Russia. [6]National University of Science and Technology "MISiS", Moscow 119049, Russia. Correspondence and requests for materials should be addressed to S.-G.J. (email: prosgjung@gmail.com) or T.P. (email: tp8701@skku.edu)

flux lines have a normal state within the core, they tend to be pinned at defects where superconductivity is suppressed, i.e., extrinsic pinning effects.

Another possible approach to improve the J_c is associated with an intrinsic property of materials, e.g., a coexisting order with superconductivity as an intrinsic pinning source. Recently, it has been proposed that magnetism may be conducive to holding the vortex, which leads to the enhancement of the J_c (refs 6–11). Several high-T_c superconductors, such as $La_{2-x}Sr_xCuO_4$ and $Ba(Fe_{1-x}Co_x)_2As_2$, are candidate materials for the intrinsic pinning because superconductivity occurs in the vicinity of an antiferromagnetically ordered state[6–8]. Superconductivity in those materials, however, requires a chemical substitution that inherently induces defects or site disorder, intertwining the effects of impurities and intrinsic pinning on J_c. In addition, it is still controversial if the magnetic order arises from macroscopically phase separated domains or from an intrinsic coexisting phase on a microscopic level. Therefore, in order to clarify the role of the intrinsic pinning on J_c, it is crucial to perform a systematic study on a high-T_c compound that is superconducting in stoichiometric form and tunable between superconducting and magnetic ground states by non-thermal control parameters.

The binary high-T_c superconductor FeSe is a promising candidate to probe the effects of the intrinsic pinning and the T_c on the J_c, because superconductivity which appears at ~10 K without introducing a hole or electron in the parent compound is greatly tunable up to 37 K by application of pressure[12,13]. In addition, an emergence of magnetic state at pressure ~0.8 GPa makes it a more interesting material in its basic properties and application issues[14,15]. A T_c above 100 K in FeSe monolayer shows its promising potential for the possibility of application[16]. In the following, we report the evolution of the critical current density (J_c) of FeSe single crystals as a function of pressure in connection with the increase of T_c.

The current-voltage ($I-V$) characteristic curves as well as temperature dependences of the electrical resistivity show a sharp contrast across the critical pressure ($P_c = 0.8$ GPa) above which μSR measurements reported a pressure-induced AFM state that coexists with superconductivity[14,15]. There are a few interesting behaviours. First, the superconducting (SC) transition is sharp at low pressures, but becomes broader in the coexisting SC state for $P > P_c$. Secondly, temperature dependence of the critical current density follows the prediction by the δT_c-pinning at low pressures ($P < P_c$), while the δl-pinning becomes more effective at higher pressures. Thirdly, amplitude of J_c is strongly enhanced in the coexisting state. The fact that physical pressure does not induce extra disorder suggests that the enhancement in J_c as well as the change in the pinning mechanism in the coexisting phase arises from the antiferromagnetically ordered state.

Results

Figure 1(a,b) representatively shows the in-plane electrical resistivity (ρ_{ab}) of FeSe as a function of temperature for several pressures. For clarity, $\rho_{ab}(T)$ for different pressures was rigidly shifted upwards. At ambient pressure, a change in the slope of ρ_{ab} occurs at 75 K due to the tetragonal to orthorhombic structural phase transition. Unlike other iron-based superconductors, this structural transition is not accompanied by a magnetic phase transition. The structural transition temperature (T_s), which is assigned as a dip in $d\rho_{ab}/dT$, progressively decreases with increasing pressure at a rate of −36.7 K/GPa and is not observable for pressures above 1.3 GPa where T_s becomes equal to the superconducting transition temperature T_c, as shown in Fig. 1(d). With further increasing pressure, an additional feature appears in the normal state as a dip or a slope change in $d\rho_{ab}/dT$, as shown in Fig. 1(e). In contrast to T_s, this new characteristic temperature linearly increases with pressure and is nicely overlaid with the T_N determined from μSR results[14], showing that the resistivity anomaly arises from the paramagnetic to antiferromagnetic phase transition, as described in Fig. 1(f).

Figure 1(c) presents that the temperature for the onset of the superconducting transition ($T_{c,on}$) gradually increases with increasing pressure at a rate of 8 K/GPa. Also, the transition width ΔT_c, which was defined as the difference between the 90 and 10% resistivity values of the normal state at $T_{c,on}$, decreases with increasing pressure at low pressures because of the enhanced superconductivity under pressure. At pressures $P > 0.8$ GPa, where superconductivity coexists with a magnetically ordered state on a microscopic scale[14,15], ΔT_c becomes broader even though $T_{c,on}$ increases with increasing pressure. The dichotomy between $T_{c,on}$ and ΔT_c in the coexisting phase suggests that the pressure-induced antiferromagnetic phase acts as an additional source for breaking Cooper pairs.

Correlation between the anomalous broadening in the ΔT_c and the magnetic phase is further supported by a qualitative difference in the current-voltage ($I-V$) curves of FeSe across the critical pressure P_c. As shown in Fig. 2(a–d), the voltage curve sharply decreases with decreasing current at 0.41 GPa, i.e., the pressure where superconductivity itself only exists. In the coexisting phase ($P > P_c$), on the other hand, the voltage curve develops a knee with decreasing current. Figure 2(d) summarizes pressure evolution of the transition broadening in the $I-V$ curve at 7 K. These anomalous broadenings in the $I-V$ curves are also considered due to the pressure-induced antiferromagnetic state.

Discussion

Two characteristic critical currents, I_c and I_f from the $I-V$ curves, are marked by the two arrows in Fig. 2(d). The depinning critical current (I_c) was obtained from the 1 μV criterion where the vortices start to move and the free-flux-flow (FFF) current (I_f) was obtained from the point where vortices are no longer affected by the pinning sites and therefore move freely[10,17]. Figure 3(a,b) describes the

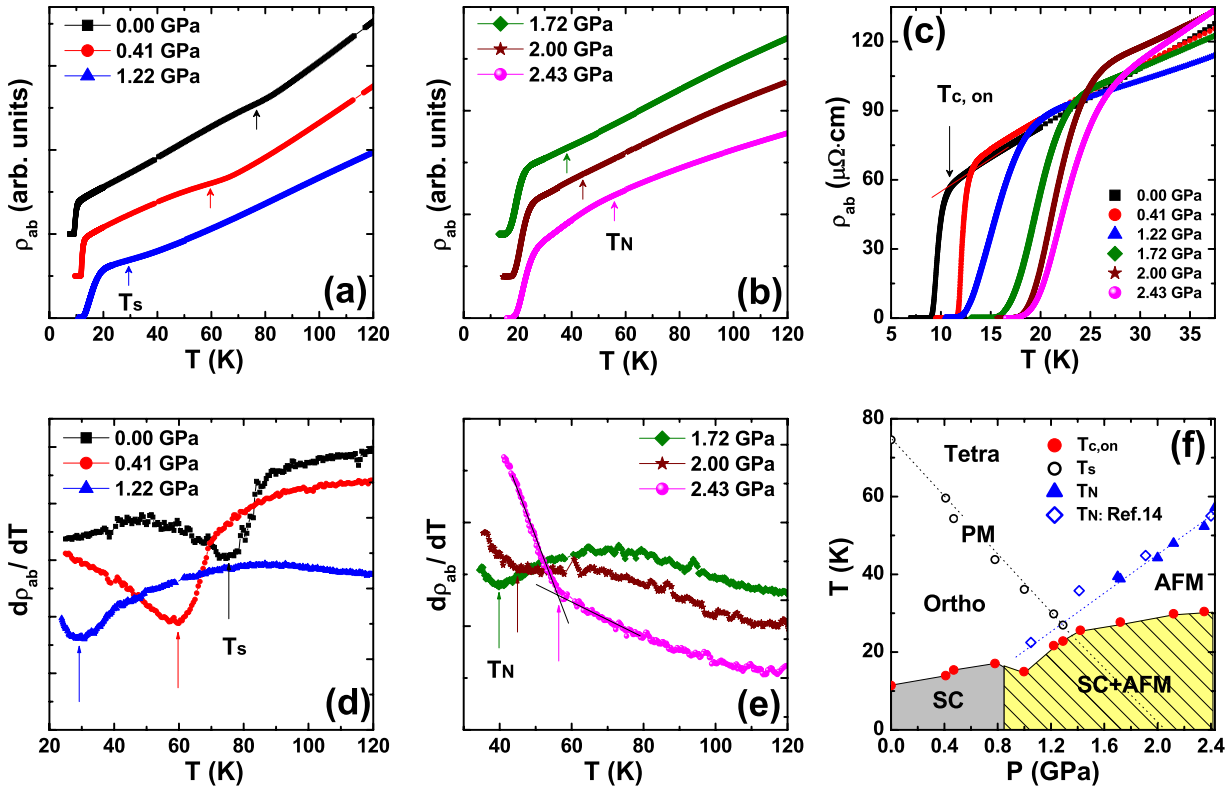

Figure 1. Electrical resistivity and phase diagram of FeSe single crystals. (**a**,**b**) In-plane electrical resistivity (ρ_{ab}) is plotted as a function of temperature for selective pressure. Arrows mark the structural (T_s) and antiferromagnetic phase transition (T_N) in (**a**,**b**), respectively. ρ_{ab} for different pressures was rigidly shifted upwards for clarity. (**c**) ρ_{ab} is magnified near the superconducting transition region, where $T_{c,on}$ is defined as the onset temperature of the SC phase transition. (**d**,**e**) First temperature derivative of the resistivity is shown as a function of temperature. Arrows mark T_s and T_N in (**d**,**e**), respectively. (**f**) Temperature-pressure phase diagram of FeSe. SC, AFM, and PM stand for superconducting, antiferromagnetic, and paramagnetic phase, respectively. Tetra and Ortho are the acronym of tetragonal and orthorhombic crystal structure.

temperature dependence of the critical current densities J_f and J_c estimated from I_f and I_c, respectively. Both J_f and J_c were significantly improved with increasing pressure. The FFF current density $J_f(T)$, which is concerned with thermally activated flux flow with increasing $T_{c,on}$, is best explained by the empirical relation $J_f(T) \sim [1-(T/T_{c,on})^n]$, with $n = 2.6 \pm 0.2$ indicated by solid lines in Fig. 3(a). The curves all collapse onto a single curve, as shown in Fig. 3(c), which cannot be explained by the depairing current density (J_d) given by $J_d(t) \propto (1-t^2)^{3/2}(1+t^2)^{1/2}$ (dashed line)[18], nor by the Joule heating, $J_{heating}$ ($\Delta T \propto J^2$) which is caused by the contact resistance (dotted line)[19]. Rather, they collapse onto the curve expected from the δT_c-pinning mechanism (solid line), $J_f(t) \propto (1-t^2)^{7/6}(1+t^2)^{5/6}$, suggesting that the temperature dependence of the FFF current density is primarily determined by spatial variations in T_c (refs 20,21).

Figure 3(b) shows the pressure evolution of the depinning critical current density (J_c), usually called the critical current density, as a function of temperature. At 1.8 K, the lowest temperature measured, J_c increases in commensurate with $T_{c,0}$ with increasing pressure, while J_c in the coexisting phase is strongly enhanced from 1.89 kA/cm^2 at 0.41 GPa (red circles) to 3.24 kA/cm^2 at 1.22 GPa (blue triangles). Here, we used the zero-resistivity SC transition temperature ($T_{c,0}$) with applied current density (J) ~ 1 A/cm^2. Resistance is not zero any more above the J_c where vortices start to move, which is significantly influenced on the pinning properties of samples, such as pinning strength, density of pinning sites, and so on. Therefore, the J_c comparison by the $T_{c,0}$ is reasonable than the comparison by the $T_{c,on}$. Considering that the increase in $T_{c,0}$ is negligible at 1.2 GPa, the anomalous jump in J_c as shown in Fig. S1 in SI, deviates from the trend in J_c as a function of $T_{c,0}$, underlining that an additional source of pinning is indeed required to explain this anomaly. The possibility of the enhancement in J_c due to improved grain boundary connectivity has been reported in some high-T_c cuprate superconductors[22,23] or in the iron-based polycrystalline superconductor $Sr_4V_2O_6Fe_2As_2$ (ref. 24). Because the studied FeSe samples are single crystalline specimens, however, the lack of a weak-link behaviour in the field dependence of J_c rules out the possibility of grain boundary as the additional pinning source (see Fig. S2 in SI). Rather, the simultaneous enhancement in J_c and appearance of antiferromagnetism indicate that the

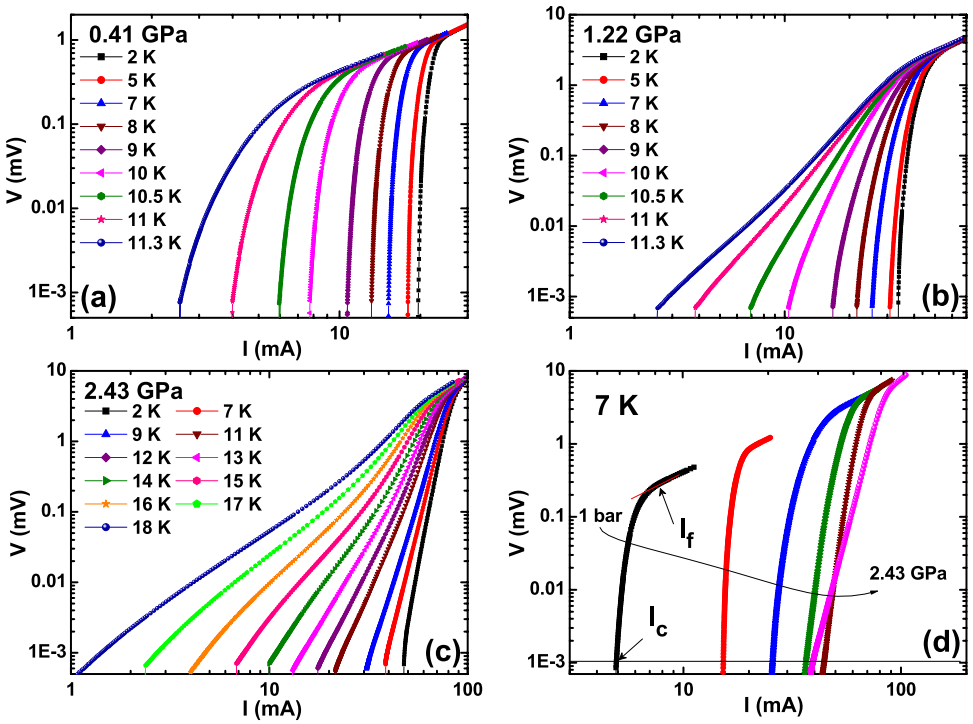

Figure 2. Evolution of transport properties of FeSe single crystals under pressure. (**a**–**c**) Logarithmic plots of the current-voltage ($I-V$) results at pressures of 0.41, 1.22 and 2.43 GPa. The $I-V$ curves become broader at pressure above 0.8 GPa, where an AFM phase is induced. (**d**) Pressure evolution of the isothermal $I-V$ curves at 7 K. The depinning critical current (I_c) is estimated by using the criterion of 1 μV, and the free-flux-flow critical current (I_f) is the value of the current at the inflection point, both of which are denoted by arrows.

pressure-induced magnetic state leads to an inhomogeneous SC phase and is conducive to the trapping of magnetic flux lines. With further increase in pressure, both J_c and $T_{c,0}$ increase.

The additional flux pinning caused by the antiferromagnetic (AFM) order in the FeSe is reflected in the different temperature dependence of J_c across the critical pressure P_c. As shown in Fig. 3(d), the normalized self-field critical current density $J_c(t_0)$ as a function of the reduced temperature ($t_0 = T/T_{c,0}$) is well described by the δT_c-pinning mechanism (solid line) for $P < P_c$, where the T_c fluctuates due to defects, such as Se deficiencies and point defects, which are the main sources for trapping the vortices. For $P \geq P_c$, however, $J_c(t_0)$ shows a completely different behaviour: the curvature of J_c near $T_{c,0}$ is positive, while it is negative at lower pressures. Also with increasing pressure, J_c deviates further away from the δT_c-pinning and at 2.43 GPa becomes close to the curve predicted by δl-pinning (dashed line), $J_c(t) \propto (1-t^2)^{5/2}(1+t^2)^{-1/2}$, suggesting that spatial fluctuations in the mean free path (l) of the charge carrier becomes important for flux pinning at high pressures[21]. As shown in Fig. S3 in SI, the pressure-induced crossover in $J_c(T)$ is almost independent of the magnetic field, indicating that the vortex pinning within the AFM phase is robust against variations in the magnetic field strength.

A similar crossover from δT_c-pinning to δl-pinning has been reported in MgB_2 when additional pinning sources, such as grain boundaries or inclusions of nanoparticles by chemical doping, were introduced[25] or hydrostatic pressure was applied[26]. In the present study, a broadening of superconducting transition with the pressure-induced AFM state is important for the crossover. A possibility of enhanced mean free path ($l \propto \xi$) fluctuations due to the competition between superconducting and AFM order parameters and change in the superconducting coherence length (ξ) with pressure may be closely related to the crossover because the disorder parameter that characterizes the collective vortex pinning properties is proportional to ξ and to $1/\xi^3$ for δT_c- and δl-pinning, respectively[21,26]. As shown in Fig. S4 in SI, the values of the upper critical field $H_{c2}(0)$ increase with applied pressure, indicating that the change in ξ may be of some relevance to the crossover.

Figure 4(a) shows a contour plot of the free-flux-flow current density (J_f) for FeSe as a function of temperature and pressure at zero field, where the colours represent different values of J_f. Also plotted are the structural and the magnetic phase boundaries that are obtained from the electrical resistivity measurements; these boundaries are consistent with those reported in previous works[14,15]. The contour of J_f monotonically increases with an increase in T_c by pressure, while J_c deviates from the monotonic pressure evolution of J_f. Instead, the contour of J_c reflects the appearance of the pressure-induced AFM

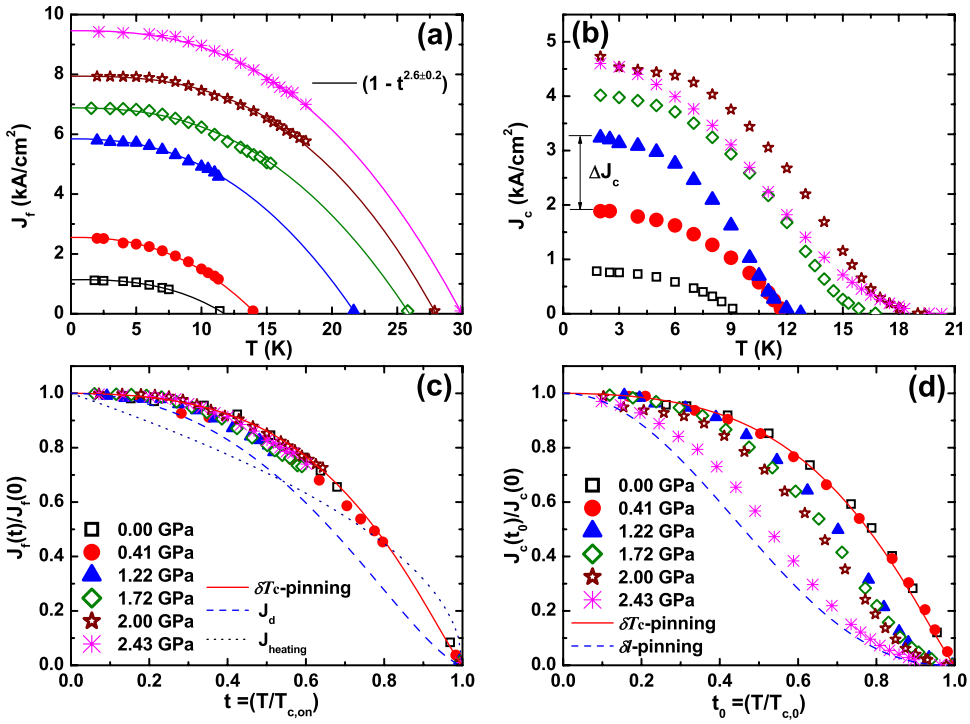

Figure 3. Critical current densities of FeSe and the flux pinning mechanism under pressure. (**a**,**b**) The free-flux-flow critical current density $J_f(T)$ monotonically increases with increasing $T_{c,on}$ by pressure and is well explained by the relation $1-(T/T_{c,on})^{2.6\pm0.2}$ over the entire pressure ranges (solid lines). On the other hand, the depinning critical current density $J_c(T)$ reveals a large enhancement at 1.22 GPa (solid triangles) even though the $T_{c,0}$ is similar to the value at 0.41 GPa (solid circles). ΔJ_c is the jump in the critical current density at 1.22 GPa, which accounts for about 70% increase from that at 0.41 GPa. (**c**) Normalized $J_f(t)$ is plotted as a function of the reduced temperature t $(=T/T_{c,on})$ for several pressures. All the curves collapse together, indicating that the underlying mechanism for the J_f is independent of enhanced $T_{c,on}$ by pressure. The $J_f(t)$ curves follow the prediction by δT_c-pinning (solid line) – see the text for detailed discussion. (**d**) Normalized $J_c(t_0)$ is plotted as a function of another reduced temperature t_0 $(=T/T_{c,0})$, where $T_{c,0}$ is the zero-resistance transition temperature. $J_c(t_0)$ closely follows the prediction from δT_c-pinning at low pressures, while it deviates from δT_c-pinning at pressures above a critical pressure (=0.8 GPa), above which a magnetic state is induced. With further increase in pressure, $J_c(t_0)$ crosses into a region where δl-pinning dominates its temperature dependence.

phase, as shown in Fig. 4(b). The J_c as well as the $T_{c,0}$ gradually increases with increasing pressure, however near the critical pressure where AFM phase is induced, J_c shows a high increase compared to $T_{c,0}$, as mentioned in Fig. 3(b). We note that J_c shows a dome shape centred around 2.1 GPa, the projected critical pressure where the tetragonal to orthorhombic structural phase transition temperature is extrapolated to $T=0$ K inside the dome of superconductivity[27]. A Possibility of flux pinning by structure transition had been reported in the superconducting A15 compounds such as V_3Si (refs 28,29), and further work is in progress to better understand the role of structural fluctuations in producing the peak in J_c.

Conclusions

In conclusion, we studied the correlation between superconducting transition temperature and critical current density for the high-T_c superconductor FeSe. Both $T_{c,on}$ and J_f increase with pressure, which is insensitive to the presence of AFM states, on the other hand, the superconducting transition width becomes considerably broader with the emergence of the AFM phase, and J_c is prominently enhanced in the coexisting phase. This behaviour reflects that the AFM phase not only provides an additional source of vortex pinning, but also makes the system susceptible to the inhomogeneous SC phase. Even though these observations are only specific to FeSe, they are expected to guide theoretical as well as experimental efforts to better understand the vortex pinning in the high-T_c superconductors where competing orders coexist on a microscopic scale. Further, when combined with well-known extrinsic pinning techniques, intrinsic magnetic pinning will provide a blueprint for greatly enhancing the critical current density, thereby bringing one step closer to the technological applications of high-temperature superconductors.

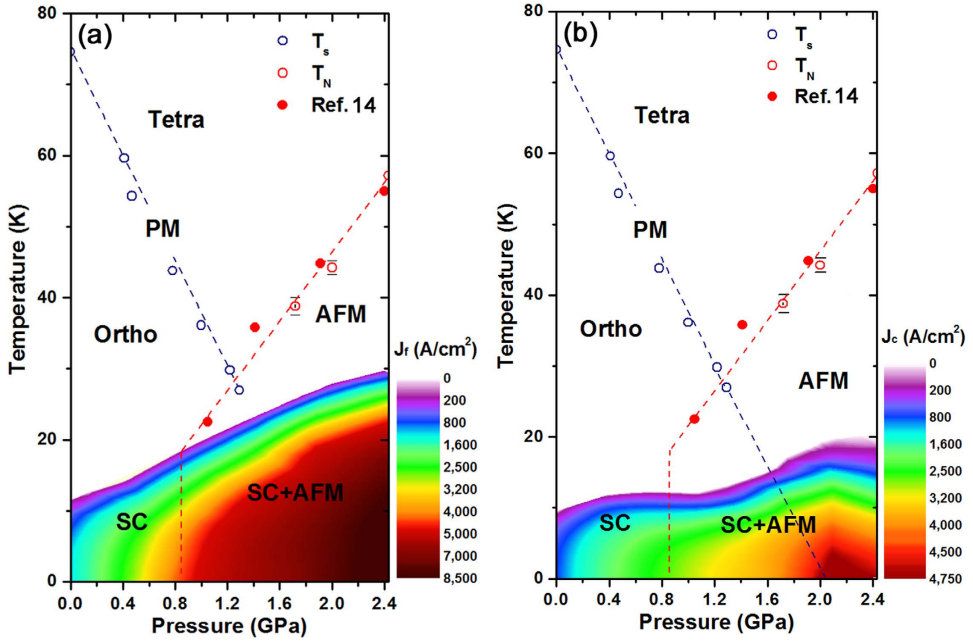

Figure 4. Phase diagram of the critical current densities, J_f and J_c. (**a**) The free-flux-flow critical current density (J_f), above which vortices flow freely, is plotted as a function of temperature and pressure. Here, the colour represents the absolute value of J_f. The magnetic and the superconducting (SC) transition temperatures based on the resistivity measurements are also plotted. For reference, we show the phase transition temperature from paramagnetic (PM) to antiferromagnetic (AFM) states based on the μSR measurements in ref. 14 (solid red circles). (**b**) A contour map of the depinning critical current density (J_c) is plotted as a function of temperature and pressure, where the colour represents the absolute value of J_c.

Methods

The *c*-axis-oriented high-quality $FeSe_{1-\delta}$ ($\delta = 0.04 \pm 0.02$) single crystals with a tetragonal structure (space group *P*4/*nmm*) were synthesised in evacuated quartz tubes in permanent gradient of temperature by using an $AlCl_3$/KCl flux. The synthesis technique used to fabricate the FeSe single crystals and their high-quality are described in detail elsewhere[30,31]. The current-voltage ($I-V$) characteristics of FeSe were measured under hydrostatic pressures of 0.00, 0.41, 1.22, 1.72, 2.00, and 2.43 GPa. The physical pressure was applied by using a hybrid clamp-type pressure cell with Daphne 7373 as the pressure-transmitting medium, and the value of the pressure at low temperatures was determined by monitoring the shift in the T_c of high-purity lead (Pb) as a manometer. The $I-V$ characteristic measurements under pressure were performed in the physical property measurement system (PPMS 9T, Quantum Design), where the electrical current was generated by using an Advantest R6142 unit and the voltage was measured by using an HP34420A nanovoltmeter. The depinning critical current (I_c) was obtained from the 1 μV criterion instead of 1 μV/cm in the $I-V$ curves due to a small size of FeSe single crystals[10,32]. A few layers of FeSe in the FeSe single crystals were easily exfoliated by using adhesive tape, which is similar to the exfoliation technique that is used for graphene[33]. The size of the measured crystals is typically $590 \times 210 \times 5\ \mu m^3$. Quasi-hydrostatic pressure was achieved by using a clamp-type piston-cylinder pressure cell with Daphne oil 7373 as the pressure-transmitting medium. The magnetic fields were applied parallel ($H//ab$) to the *ab*-plane of the samples.

References

1. Nishijima, S. *et al.* Superconductivity and the Environment: a Roadmap. *Supercond. Sci. Technol.* **26,** 113001 (2013).
2. Hull, J. R. Applications of High-temperature Superconductors in Power Technology. *Rep. Prog. Phys.* **66,** 1865–1886 (2003).
3. Larbalestier, D. C., Gurevich, A., Feldmann, D. M. & Polyanskii, A. High-T_c Superconducting Materials for Electric Power Applications. *Nature* **414,** 368–377 (2001).
4. Baert, M., Metlushko, V. V., Jonckheere, R., Moshchalkov, V. V. & Bruynseraede, Y. Composite Flux-line Lattices Stabilized in Superconducting Films by a Regular Array of Artificial Defects. *Phys. Rev. Lett.* **74,** 3269–3272 (1995).
5. Civale, L. *et al.* Vortex Confinement by Columnar Defects in $YBa_2Cu_3O_7$ Crystals: Enhanced Pinning at High Fields and Temperatures. *Phys. Rev. Lett.* **67,** 648–651 (1991).
6. Zaanen, J. Superconductivity: Technology meets quantum criticality. *J. Nature Mater.* **4,** 655–656 (2005).
7. Prozorov, R. *et al.* Coexistence of Long-range Magnetic Order and Superconductivity from Campbell Penetration Depth Measurements. *Supercond. Sci. Technol.* **22,** 034008 (2000).
8. Prozorov, R. *et al.* Intrinsic Pinning on Structural Domains in Underdoped Single Crystals of $Ba(Fe_{1-x}Co_x)_2As_2$. *Phys. Rev. B* **80,** 174517 (2009).

9. Gammel, P. L. *et al.* Enhanced Critical Currents of Superconducting $ErNi_2B_2C$ in the Ferromagnetically Ordered State. *Phys. Rev. Lett.* **84,** 2497–2500 (2000).
10. Weigand, M. *et al.* Strong Enhancement of the Critical Current at the Antiferromagnetic Transition in $ErNi_2B_2C$ Single Crystals. *Phys. Rev. B* **87,** 140506(R) (2013).
11. Refal, T. F. Antiferromagnetism and Enhancement of Superconductivity. *Supercond. Sci. Technol.* **2,** 149–152 (1989).
12. Hsu, F. C. *et al.* Superconductivity in the PbO-type Structure α-FeSe. *Proc. Natl. Acad. Sci. (USA)* **105,** 14262 (2008).
13. Mizuguchi, Y., Tomioka, F., Tsuda, S., Yamaguchi, T. & Takano, Y. Superconductivity at 27 K in Tetragonal FeSe under High Pressure. *Appl. Phys. Lett.* **93,** 152505 (2008).
14. Bendele, M. *et al.* Coexistence of Superconductivity and Magnetism in $FeSe_{1-x}$ under Pressure. *Phys. Rev. B* **85,** 064517 (2012).
15. Bendele, M. *et al.* Pressure Induced Static Magnetic Order in Superconducting $FeSe_{1-x}$. *Phys. Rev. Lett.* **104,** 087003 (2010).
16. Ge, J. F. *et al.* Superconductivity above 100 K in Single-Layer FeSe Films on Doped $SrTiO_3$. *Nat. Mater.* **14,** 285–289 (2015).
17. Gupta, S. K. *et al.* $I-V$ Characteristic Measurements to Study the Nature of the Vortex State and Dissipation in MgB_2 Thin Films. *Phys. Rev. B* **66,** 104525 (2002).
18. Kunchur, M. N., Lee, S.-I. & Kang, W. N. Pair-breaking Critical Current Density of Magnesium Diboride. *Phys. Rev. B* **68,** 064516 (2003).
19. Xiao, Z. L., Andrei, E. Y., Shuk, P. & Greenblatt, M. Joule Heating Induced by Vortex Motion in a Type-II Superconductor. *Phys. Rev. B* **64,** 094511 (2001).
20. Blatter, G., Feigel'man, M. V., Geshkenbein, V. B., Larkin, A. I. & Vinokur, V. M. Vortices in High-temperature Superconductors. *Rev. Mod. Phys.* **66,** 1125–1388 (1994).
21. Griessen, R. *et al.* Evidence for Mean Free Path Fluctuation Induced Pinning in $YBa_2Cu_3O_7$ and $YBa_2Cu_4O_8$ Films. *Phys. Rev. Lett.* **72,** 1910–1913 (1994).
22. Tomita, T., Schilling, S., Chen, L., Veal, B. W. & Claus, H. Enhancement of the Critical Current Density of $YBa_2Cu_3O_x$ Superconductors under Hydrostatic Pressure. *Phys. Rev. Lett.* **96,** 077001 (2006).
23. Bud'ko, S. L., Davis, M. F., Wolfe, J. C., Chu, C. W. & Hor, P. H. Pressure and Temperature Dependence of the Critical Current Density in $YBa_2Cu_3O_{7-\delta}$ Thin Films. *Phys. Rev. B* **47,** 2835–2839 (1993).
24. Shabbir, B. *et al.* Hydrostatic Pressure: A Very Effective Approach to Significantly Enhance Critical Current Density in Granular Iron Pnictide Superconductors. *Sci. Rep.* **5,** 8213 (2015).
25. Ghorbani, S. R., Wang, X. L., Hossain, M. S. A., Dou, S. X. & Lee, S.-I. Coexistence of the δl and δT_c Flux Pinning Mechanisms in Nano-Si-doped MgB_2. *Supercond. Sci. Technol.* **23,** 025019 (2010).
26. Shabbir, B., Wang, X. L., Ghorbani, S. R., Dou, S. X. & Xiang, F. Hydrostatic Pressure Induced Transition from δT_c to $\delta \ell$ Pinning Mechanism in MgB_2. *Supercond. Sci. Technol.* **28,** 055001 (2015).
27. Miyoshi, K. *et al.* Enhanced superconductivity on the tetragonal lattice in FeSe under hydrostatic pressure. *J. Phys. Soc. Jpn.* **83,** 013702 (2014).
28. Dew-Hughes, D. Flux Pinning Mechanisms in Type-II Superconductors. *Phil. Mag.* **30,** 293–305 (1974).
29. Brand, R. & Webb, W. W. Effects of Stress and Structure on Critical Current Densities of Superconducting V_3Si. *Solid State Commun.* **7,** 19–21 (1969).
30. Chareev, D. *et al.* Single Crystal Growth and Characterization of Tetragonal $FeSe_{1-x}$ Superconductors. *CrystEngComm* **15,** 1989–1993 (2013).
31. Lin, J.-Y. *et al.* Coexistence of Isotropic and Extended s-wave Order Parameters in FeSe as revealed by Low-temperature Specific Heat. *Phys. Rev. B* **84,** 220507(R) (2011).
32. Li, G., Andrei, E. Y., Xiao, Z. L., Shuk, P. & Greenblatt, M. Onset of Motion and Dynamic Reordering of a Vortex Lattice. *Phys. Rev. Lett.* **96,** 017009 (2006).
33. Novoselov, K. S. *et al.* Electric Field Effect in Atomically Thin Carbon Films. *Science* **306,** 666–669 (2004).

Acknowledgements

We thank W. N. Kang, S. Lin, and J. D. Thompson for helpful discussions. This work was supported by the National Research Foundation (NRF) of Korea grant funded by the Korean Ministry of Science, ICT and Planning (No. 2012R1A3A2048816). This work was supported in part by the Ministry of Education and Science of the Russian Federation within the framework of the Increase Competitiveness Program of the National University of Science and Technology "MISiS" (Contract No. K2-014-036).

Author Contributions

S.-G.J., J.-H.K., E.P. and S.L. performed the $I-V$ measurements at various pressures. D.A.C., J.-Y.L. and A.N.V. provided the FeSe single crystals. S.-G.J. and J.-H.K. analysed the data and discussed the results with all authors. The manuscript was written by S.-G.J. and T.P. with inputs from all authors.

Additional Information

Supplementary information accompanies this paper at http://www.nature.com/srep

Competing financial interests: The authors declare no competing financial interests.

How to cite this article: Jung, S.-G. *et al.* Enhanced critical current density in the pressure-induced magnetic state of the high-temperature superconductor FeSe. *Sci. Rep.* **5**, 16385; doi: 10.1038/srep16385 (2015).